# Mice generated by in vitro fertilization exhibit vascular dysfunction and shortened life span

Emrush Rexhaj,[1] Ariane Paoloni-Giacobino,[2] Stefano F. Rimoldi,[1] Daniel G. Fuster,[3] Manuel Anderegg,[3] Emmanuel Somm,[4] Elisa Bouillet,[1] Yves Allemann,[1] Claudio Sartori,[1,5] and Urs Scherrer[1,6]

[1]Swiss Cardiovascular Center Bern and Department of Clinical Research, University Hospital, Bern, Switzerland. [2]Department of Genetic and Laboratory Medicine and Swiss Center for Applied Human Toxicology, Geneva University Hospital, Geneva, Switzerland. [3]Division of Nephrology, Hypertension and Clinical Pharmacology, University Hospital, Bern, Switzerland. [4]Division of Development and Growth, Department of Paediatrics, University of Geneva Medical School, Geneva, Switzerland. [5]Department of Internal Medicine, CHUV, Lausanne, Switzerland. [6]Facultad de Ciencias, Departamento de Biología, Universidad de Tarapacá, Arica, Chile.

**Children conceived by assisted reproductive technologies (ART) display a level of vascular dysfunction similar to that seen in children of mothers with preeclamspia. The long-term consequences of ART-associated vascular disorders are unknown and difficult to investigate in healthy children. Here, we found that vasculature from mice generated by ART display endothelial dysfunction and increased stiffness, which translated into arterial hypertension in vivo. Progeny of male ART mice also exhibited vascular dysfunction, suggesting underlying epigenetic modifications. ART mice had altered methylation at the promoter of the gene encoding eNOS in the aorta, which correlated with decreased vascular eNOS expression and NO synthesis. Administration of a deacetylase inhibitor to ART mice normalized vascular gene methylation and function and resulted in progeny without vascular dysfunction. The induction of ART-associated vascular and epigenetic alterations appeared to be related to the embryo environment; these alterations were possibly facilitated by the hormonally stimulated ovulation accompanying ART. Finally, ART mice challenged with a high-fat diet had roughly a 25% shorter life span compared with control animals. This study highlights the potential of ART to induce vascular dysfunction and shorten life span and suggests that epigenetic alterations contribute to these problems.**

## Introduction

Epidemiological studies showing an association between pathologic events during early life and the development of cardiovascular and metabolic disease in adulthood have led to the "fetal programming of adult disease hypothesis" (1, 2). In line with this hypothesis, experimental studies show that short-term hypoxemia after birth predisposes to exaggerated hypoxic pulmonary vasoconstriction later in life in rats (3) and humans (4) and preeclampsia predisposes the offspring to pulmonary and systemic endothelial dysfunction (5). Recent data suggest that assisted reproductive technologies (ART) represent another example for this hypothesis, since arterial pressure is increased in rats and children generated by ART (6, 7) and young children conceived by ART display generalized vascular dysfunction and signs of early arteriosclerosis (8).

While these findings demonstrate vascular dysfunction in ART children that is of magnitude similar to that observed in offspring of mothers with preeclampsia (5) or preadolescents with type I diabetes (9), conditions known to be associated with an increased risk for premature cardiovascular morbidity (10–12), several important issues remain unclear. First, in humans, it is difficult to determine whether this problem is related to the ART procedure itself or to parental factors. Second, the long-term cardiovascular consequences of ART are unknown because this population has not yet reached the age at which premature cardiovascular diseases typically start to occur. Finally, the underlying mechanisms of ART-induced vascular dysfunction are not known and are difficult to study in healthy children.

We, therefore, developed a mouse model of ART to first test the hypothesis that ART induces vascular dysfunction in the offspring of normal mice. We found that ART mice display endothelial dysfunction, increased arterial stiffness, and arterial hypertension. To study whether ART predisposes to premature mortality, we compared the life span of ART and control mice fed with normal chow or challenged with a high-fat diet (HFD). We then started to test for underlying mechanisms. Hormonal stimulation of ovulation is inherently needed for ART and may have effects on vascular function in the offspring. We, therefore, compared vascular function between mice born after hormonal stimulation in the mother and control mice. The time passed in culture medium may be another factor involved in ART-induced vascular dysfunction. To test this hypothesis, we compared vascular function between mice born after implantation of 2 cell embryos and blastocysts. Finally, in mice, epigenetic mechanism are involved in the fetal programming of vascular dysfunction (13), and in humans, the prevalence of very rare diseases caused by epigenetic mechanisms is increased in ART (14, 15). Epigenetic alterations may be transmitted to the next generation (13, 16, 17). Therefore, we examined whether male ART mice transmitted the vascular dysfunction to their progeny. In a next step, we then

**Authorship note:** Claudio Sartori and Urs Scherrer contributed equally to this work.
**Conflict of interest:** The authors have declared that no conflict of interest exists.
**Citation for this article:** *J Clin Invest.* 2013;123(12):5052–5060. doi:10.1172/JCI68943.

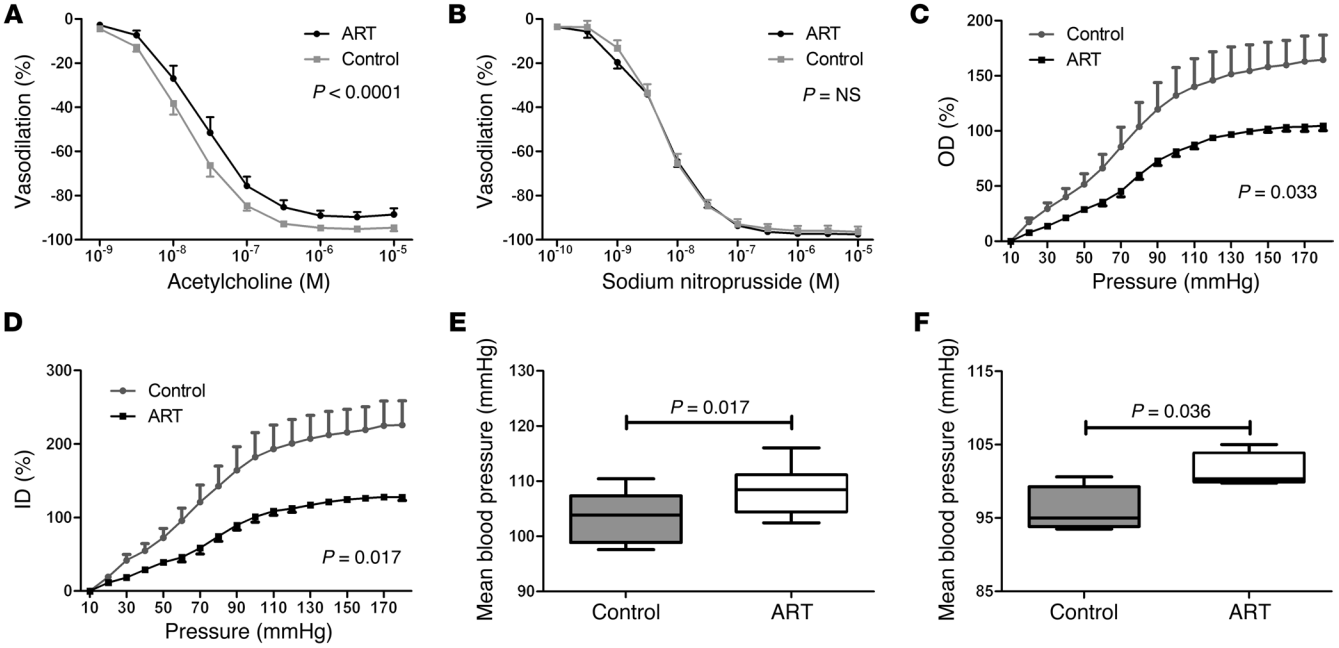


**Figure 1**
Mesenteric artery responsiveness, carotid artery pressure diameter relationship, and arterial blood pressure in mice generated by ART and control mice. (**A**) Acetylcholine-induced and (**B**) sodium nitroprusside–induced mesenteric artery vasodilation in vitro (data represent mean ± SEM). (**C** and **D**) Carotid artery pressure diameter relationship in vitro. **C** shows outer diameter (OD) and **D** shows inner diameter (ID). (**E**) Mean arterial blood pressure in vivo obtained by short-term measurements and (**F**) 48-hour long-term measurements by telemetry. Horizontal lines represent the median; boxes, 25th to 75th percentiles; and T bars, 5th and 95th percentiles. Data are for at least 10 mice per group except for **C** and **D** ($n$ = 5 per group) and **F** ($n$ = 4 per group).

studied the methylation of imprinted genes and genes involved in cardiovascular regulation in ART mice, offspring of ART mice, and control mice. Finally, we examined the effects of administration of a deacetylase inhibitor on the methylation of genes and vascular function in these 3 groups of animals.

## Results

### *Endothelial dysfunction, increased arterial stiffness, and arterial hypertension in ART mice*

To assess the putative effects of ART on vascular function, we assessed acetylcholine-mediated and nitroprusside-induced mesenteric artery vasodilation in vitro in ART and control mice. We found that acetylcholine-induced vasodilation was impaired in ART mice compared with control mice (Figure 1A). In contrast, nitroprusside-induced vasodilation was normal in ART mice (Figure 1B), demonstrating mesenteric artery endothelial dysfunction. To assess for premature vascular senescence, we examined carotid artery vascular stiffness. We found that vascular stiffness was increased in ART mice (Figure 1, C and D). To examine whether endothelial dysfunction in vitro had functional consequences in vivo, we measured arterial blood pressure and found that it was higher in ART mice than in control mice, both during short-term measurements and during chronic measurements by telemetry over 48 hours (Figure 1, E and F).

### *Decreased life span in ART mice*

To evaluate whether ART had consequences on the life span in mice, we compared the survival of ART and control mice. To facilitate the detection of potential differences, in addition to groups of mice fed with normal chow, groups of ART and control mice were challenged with a HFD. We found that in mice fed with normal chow, life span was similar in the 2 groups. In contrast, a HFD, while not having a detectable effect on life span in control mice, significantly reduced survival in ART mice ($P$ < 0.0001, Figure 2).

### *Underlying mechanisms*

*Effects of stimulation of the ovulation in the mother on vascular function in the offspring.* To examine whether hormonal stimulation of ovulation in the mother alters vascular function in the offspring, we

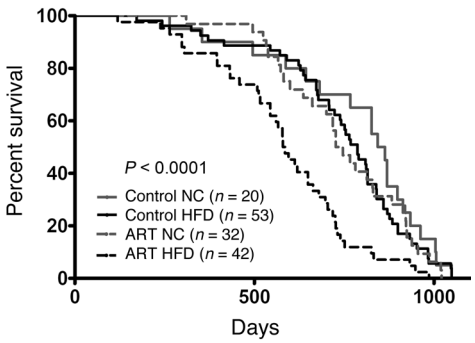


**Figure 2**
Kaplan-Meier survival curves of ART and control mice fed with normal chow (NC) or challenged with a HFD. Median survival (days): Control NC = 853; control HFD = 787; ART normal chow = 736; ART HFD = 582.

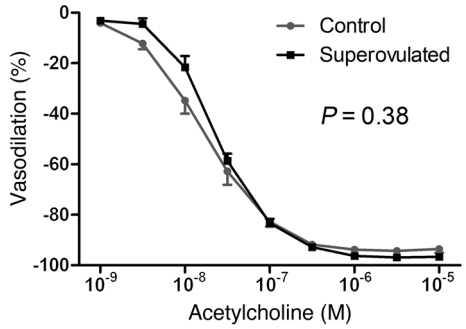


**Figure 3**
Acetylcholine-induced mesenteric artery vasodilation in vitro in offspring of superovulated and control mice. Data represent mean ± SEM for at least 7 mice per group.

compared mesenteric artery responses to acetylcholine in offspring of superovulated and control mice. Overall, acetylcholine-induced mesenteric vasodilation was comparable in the 2 groups (Figure 3), but at lower doses of acetylcholine, curves tended to diverge, and the responses to the $1 \times 10^{-8}$ dose were statistically different between the 2 groups ($P = 0.04$).

*Vascular dysfunction is similar in ART mice generated by implantation of 2 cell embryos and blastocysts*. To examine whether a shorter duration of embryo culture attenuates/prevents ART-induced vascular dysfunction in the offspring, we compared mesenteric artery responses to acetylcholine and arterial blood pressure between mice generated by implantation of 2 cell embryos (30 hours of incubation) and blastocysts (96 hours of incubation). ART-induced vascular dysfunction and arterial hypertension were comparable in the 2 groups of mice (Figure 4).

*Male ART mice transmit the vascular dysfunction to their progeny*. There is evidence that ART may alter epigenetic mechanisms (14, 15). These alterations may be transmitted to the next generation (13, 16, 17). To test for this possibility, we examined vascular function and arterial blood pressure in male offspring generated by mating male ART mice with control females. Endothelial dysfunction and arterial hypertension in offspring of male ART mice were comparable to those observed in their fathers (Figure 5, A and B).

***Methylation of imprinted genes in the aorta is altered in ART mice and their progeny***

*Normalization by administration of the deacetylase inhibitor butyrate*. To evaluate whether ART altered the methylation of genes in the vasculature, we studied the methylation of imprinted genes in the aorta. We found that the methylation of the imprinted genes *H19*, *Gtl2*, and *Peg3*, but not of *Peg1* and *Snrpn*, was altered in the aorta of ART mice (Figure 6). To determine whether these alterations were specific for vascular tissue or generalized, we examined the methylation of these genes in the liver and found that it was similar in the 2 groups (data not shown). Finally, to study whether altered methylation was transmitted to the next generation, we examined the methylation of imprinted genes in the aorta of the progeny of male ART mice. The alterations of the methylation of imprinted genes in the aorta of the offspring were comparable to those observed in their fathers (Figure 6).

Deacetylase inhibitors are capable of normalizing altered methylation (13, 18). We therefore examined the effects of butyrate administration to male ART mice on the methylation of imprinted genes. We found that butyrate normalized the methylation of the imprinted genes *H19*, *Gtl2*, and *Peg3* (but had no detectable effect on the methylation of the normally methylated imprinted genes *Peg1* and *Snrpn*) in the aorta of ART mice, whereas it had no detectable effect on the methylation of these genes in control mice (all $P > 0.22$, control + vehicle vs. control + butyrate; Figure 6). Finally, butyrate administration to male ART mice before mating prevented the transmission of altered methylation to the progeny (Figure 6).

***Altered DNA methylation of the promoter of the eNOS gene, altered eNOS and eNOS mRNA expression in vascular tissue, and decreased nitric oxide plasma concentration in ART mice***

*Normalization by administration of the deacetylase inhibitor butyrate*. While the above findings show altered methylation of imprinted genes in ART mice, the consequences of these alterations are not known, since the physiologic function of these genes is unknown. We, therefore examined DNA methylation of genes known to be important in cardiovascular regulation. DNA methylation of the promoter of the eNOS gene was increased in the aorta of ART mice (Figure 7A), whereas DNA methylation of the promoter of the endothelin-1 and the angiotensin converting enzyme (ACE) gene was not different between ART and control mice (endothelin-1: 15.9% ± 1.0% vs. 16.4% ± 1.0%, control vs. ART, $P = 0.27$; ACE: 4.0% ± 0.5% vs. 3.9% ± 0.3%,

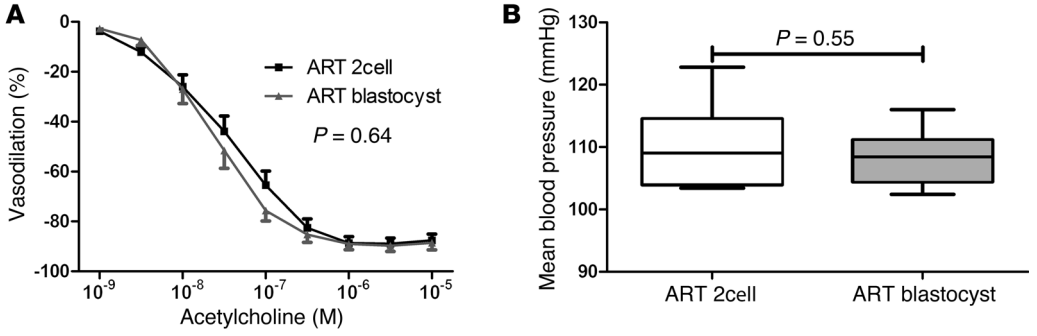


**Figure 4**
Effects of embryo culture time on mesenteric artery responsiveness and blood pressure in ART mice. Mesenteric artery responsiveness to acetylcholine (**A**) and arterial blood pressure (**B**) in ART-mice generated by implantation of 2 cell embryos and blastocysts. In **A**, data represent mean ± SE. In **B**, horizontal lines represent the median; boxes, 25th to 75th percentiles; and T bars, 5th and 95th percentiles. Data are for at least 9 mice per group.

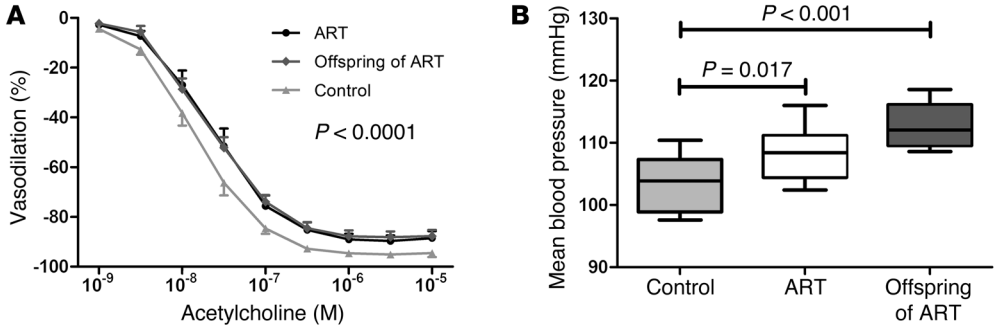


**Figure 5**

Transmission of vascular dysfunction and arterial hypertension by mice generated by ART to their offspring. Mesenteric artery responsiveness to acetylcholine in vitro (**A**) and arterial blood pressure in vivo (**B**) in mice generated by ART, offspring of mice generated by ART, and control mice. In **A**, data represent mean ± SEM. In **B** horizontal lines represent the median; boxes, 25th to 75th percentiles; and T bars, 5th and 95th percentiles. *P* values by 1-way ANOVA and Dunnett's post hoc test. Data are for at least 10 mice per group.

control vs. ART, $P = 0.33$). Increased promoter DNA methylation downregulates eNOS expression in endothelial cells in vitro (19). In line with this concept, eNOS expression (Figure 7B) and *eNOS* mRNA expression (0.56% ± 0.08% vs. 1.0% ± 1.21%, $P = 0.047$, ART vs. control) in the carotid artery were decreased in ART mice compared with control animals. Decreased eNOS expression appeared to be of functional importance, because nitric oxide ($NO_x$) plasma concentration was lower in ART than in control mice (Figure 7C).

Butyrate administration to ART mice normalized DNA methylation of the promoter of the eNOS gene (Figure 7A) and eNOS expression (Figure 7B) and restored $NO_x$ plasma concentration (Figure 7C).

*Butyrate administration to ART mice normalizes endothelial function and prevents transmission of vascular dysfunction to the offspring.* To evaluate whether normalization of the DNA methylation and vascular NO synthesis by butyrate had favorable effects on vascular function in ART mice,we examined vascular responsiveness to acetylcholine. We found that butyrate administration to ART mice normalized mesenteric artery function, whereas it had no detectable effect on this function in control mice (Figure 8A). Moreover, butyrate administration to male ART mice before mating prevented the transmission of vascular dysfunction to the next generation (Figure 8B).

## Discussion

We recently showed that children conceived by ART display vascular dysfunction (8). The long-term consequences of this problem are unknown, and its underlying mechanisms are difficult to investigate in healthy children. Here, we show for what we believe is the first time that in mice generated by ART, endothelial function of the systemic circulation in vitro is defective and translates into arterial hypertension in vivo. Moreover, ART also had consequences on the life span; when mice were challenged with a HFD, life span was roughly 25% shorter in ART than in control mice.

Consistent with findings in children conceived by ART showing endothelial dysfunction (8), in ART mice, acetylcholine-induced mesenteric artery dilation was impaired while endothelium-independent dilation was preserved. Moreover, as in ART

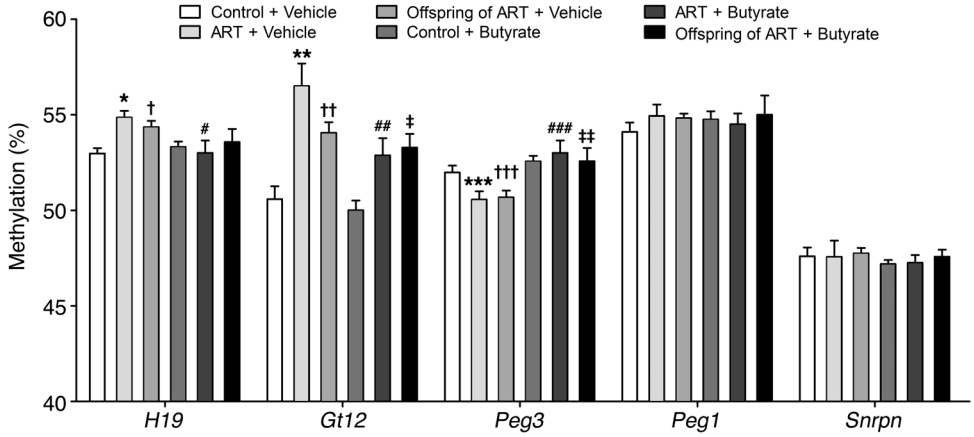


**Figure 6**

Methylation of imprinted genes *H19*, *Gtl2*, *Peg3*, *Peg1*, and *Snrpn* in the aorta of control mice, mice generated by ART, and their progeny. Effects of administration of the deacetylase inhibitor butyrate to control and ART mice on the methylation of these genes and on the transmission of the dysmethylation to the progeny. $^{*}P < 0.001$, $^{**}P < 0.001$, $^{***}P = 0.02$, ART + vehicle vs. control + vehicle; $^{\#}P = 0.03$, $^{\#\#}P = 0.03$, $^{\#\#\#}P < 0.01$, ART + butyrate vs. ART + vehicle; $^{\dagger}P < 0.01$, $^{\dagger\dagger}P < 0.001$, $^{\dagger\dagger\dagger}P = 0.014$, offspring of ART + vehicle vs. control + vehicle; $^{\ddagger}P = 0.04$,$^{\ddagger\ddagger}P = 0.03$, offspring of ART + butyrate vs. ART + vehicle. Data represent mean ± SEM for at least 7 mice per group.

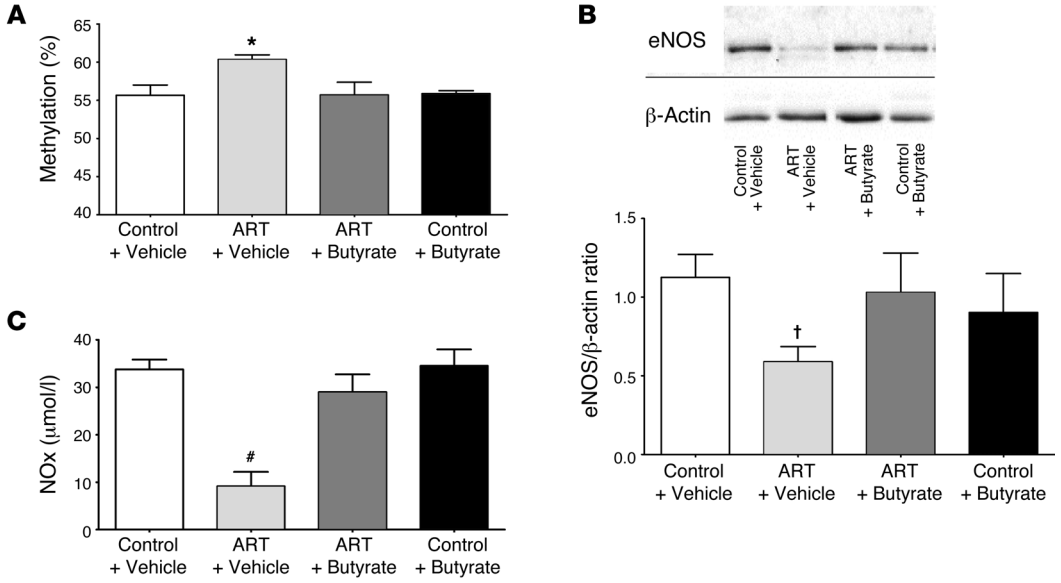


**Figure 7**
Butyrate administration to ART mice normalizes DNA promoter methylation and expression of the *eNOS* gene in vascular tissue and $NO_x$ plasma concentration. DNA methylation of the promoter of the *eNOS* gene in the aorta (**A**), eNOS expression in the carotid artery (**B**), and $NO_x$ plasma concentration (**C**), in control + vehicle, ART + vehicle, ART + butyrate, and control + butyrate mice. Data represent mean ± SEM for at least 13 mice per group. $^*P = 0.004$, $^\#P < 0.0001$, $^\dagger P = 0.03$ vs. control + vehicle by 1-way ANOVA and Dunnett's post hoc test. In **B**, the lanes were run on the same gel but were noncontiguous.

children, arterial stiffness was increased in ART mice. Whereas in young ART children, endothelial dysfunction was not associated with arterial hypertension, in adult ART mice, endothelial dysfunction in the systemic circulation was associated with arterial hypertension. In humans, it has been speculated that parental factors (e.g., older age of mothers necessitating to resort to ART, sterility-associated vascular dysfunction that is transmitted to the offspring) contribute to vascular dysfunction in offspring of ART. The present findings showing that in normal mice ART induces vascular dysfunction in the offspring indicate that ART per se is the main culprit. Data in humans showing no relationship between the age of the mother and vascular function in the offspring and demonstrating normal vascular function in sterile parents are in line with this concept (8).

Due to the young age of the ART population in humans (the first ART child was born in 1978), it is not known yet whether ART will affect life expectancy in humans. Here we found that when fed normal chow, life span was not different in ART and control mice. However, when mice were challenged with a Western style HFD, life span in ART mice was roughly 25% shorter than in control mice. Premature vascular senescence and exaggerated HFD-induced glucose intolerance and insulin resistance (20) may contribute to this problem. These effects of ART were observed in FVB mice, a mouse strain less susceptible to atherosclerosis than, for example, the C57BL/6 strain (21, 22), suggesting that the effects of IVF may have a greater impact in genetically susceptible individuals. These findings suggest that it may be worthwhile to provide dietary advice to persons born with the help of ART.

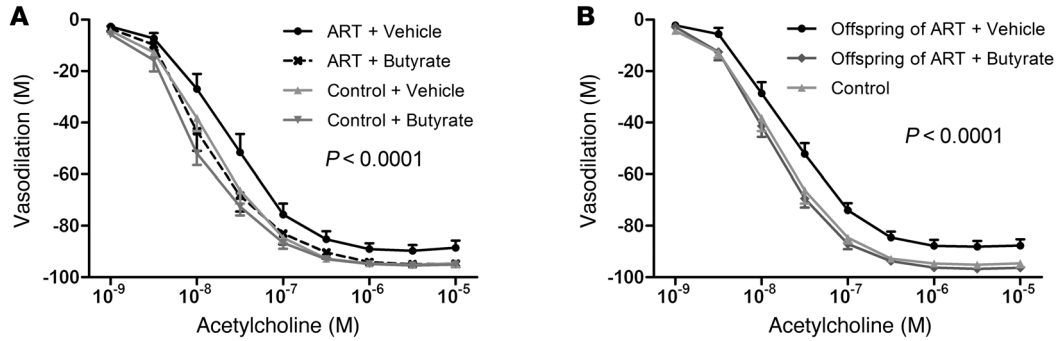


**Figure 8**
Butyrate administration to ART mice normalizes vascular function and prevents transmission of dysfunction to offspring. (**A**) Effects of butyrate administration to ART and to control mice on acetylcholine-induced mesenteric artery dilation. (**B**) Effects of butyrate or vehicle administration to ART mice before mating on acetylcholine-induced mesenteric artery dilation in the progeny. Data represent mean ± SEM for at least 10 mice per group.

In mice, fetal programming of pulmonary vascular dysfunction is associated with altered lung DNA methylation (13) and there is evidence for transmission of epigenetic alterations to the next generation. Here, we found that vascular dysfunction and arterial hypertension of the progeny of male ART mice mated with normal females was similar to what was found in their fathers. In line with this observation, the methylation of imprinted genes was altered similarly in the aorta of ART mice and their progeny. While these findings provide proof of principle for epigenetic alterations in the vasculature of ART mice, the consequences of these alterations for vascular regulation, if any, are unknown. In a next step, we, therefore, examined the methylation of genes known to be important for vascular regulation. We found that DNA methylation of the promoter of the eNOS gene was increased in arterial tissue of ART mice and associated with decreased eNOS expression, decreased *eNOS* mRNA expression, and lower $NO_x$ plasma concentration in ART than in control mice. Taken together, these findings indicate that in mice, ART alters the entire chain of events starting from altered eNOS methylation in the vasculature over endothelial dysfunction and premature vascular senescence to arterial hypertension and possibly premature mortality. Finally, the methylation of the promoter of the endothelin-1 and the *ACE* gene was not altered in ART mice, suggesting that there exist no global changes of DNA methylation of genes involved in vascular regulation.

There is increasing evidence for an interplay between histone modifications and DNA methylation in gene silencing (23). Changes of methylation can be reversed by histone deacetylase inhibitors that are known to induce replication-independent demethylation of ectopically methylated genes (13, 24, 25). Histone deacetylase inhibitors have been shown to reverse epigenetic and phenotypic changes induced by pathologic events during early life (26) and to prevent transmission of these changes to the progeny (13). In line with these observations, we found that butyrate administration to male ART mice normalized methylation and expression of the *eNOS* gene in vascular tissue together with vascular responsiveness to acetylcholine. Moreover, it prevented the transmission of vascular dysfunction to the progeny. Collectively, these data suggest that in mice, epigenetic mechanisms contribute to ART-induced vascular dysfunction.

The present studies also provide insight regarding the etiology of ART-induced cardiovascular and epigenetic alterations that may have consequences for ART in humans. Culture time and hormonal effects related to stimulation of ovulation and embryo culture per se (independent of time) are candidate mechanisms. Here, we found that the culture time needed to obtain 2-cell embryos was sufficient to cause these changes, since endothelial dysfunction and arterial hypertension were comparable in ART mice generated by implantation of 2-cell embryos and blastocysts. In humans, embryos are generally implanted at the blastocyst stage. The present findings in mice suggest that in humans, attempts to shorten the time lag between fertilization and implantation are unlikely to prevent ART-induced vascular dysfunction.

ART implies stimulation of the ovulation in the mother, and it has been speculated that this procedure may have adverse effects in the offspring (27). In line with recent findings in humans demonstrating normal vascular function in children conceived during ovarian stimulation in the mother (8), we found that endothelium-dependent mesenteric artery vasodilation was normal in offspring of superovulated mice. However, while we did not see a significant overall effect of hormonal stimulation alone on endothelial function in mice, there was a significant ($P = 0.04$) difference at a lower dose of acetylcholine between hormonally stimulated and control mice, suggesting the possibility of an additive effect between hormonal stimulation and cell culture on ART-induced epigenetic and vascular alterations in mice. In line with this speculation, epigenetic alterations in mouse embryos induced by hormonal stimulation and culture were reported to be greater than those induced by embryo culture alone (28). Current culture media used for in vitro fertilization are suboptimal, as evidenced by reduced pregnancy rates, viability, and growth of cultured compared with in vivo embryos. For example, culture media may lack or contain at different concentration key metabolites and/or growth factors present in oviductal fluid and are not capable of reproducing the dynamic changes of oviductal fluid naturally occurring along the female reproductive tract. Suboptimal in vitro culture conditions result in compromised ability to maintain genomic imprinting of in vitro compared with in vivo embryos (28) and may contribute to the observed epigenetic and cardiovascular alterations in ART mice in the present study. In line with this speculation, modification of the culture medium may allow ART-induced cardiovascular dysfunction in mice to be attenuated (29). Taken together, the present findings suggest that embryo culture per se is the main culprit underpinning ART-induced epigenetic and vascular alterations in mice. These alterations may be facilitated by hormonal stimulation of ovulation in the mother. We speculate that similar mechanisms may play a role in the rapidly growing population of humans conceived by ART, who now make up 2% to 4% of births in developed countries.

## Methods

*Chemicals and reagents*. Pregnant mare serum gonadotropin (PMSG), human chorionic gonadotropin (hCG), and ketamin were from Intervet. Human tubal fluid medium (HTF), human serum albumin (HSA), and paraffin oil were from Irvine Scientific. G1 and G2 media were from Vitrolife. Sodium butyrate, acetylcholine and sodium nitroprusside were from Sigma-Aldrich. Xylazine was from Bayer HealthCare. Temgesic (buprenorphine) was from Essex Chemie. Bactrim was from Roche. Biokema Flunixine was from Biokema SA.

*Animals*. Wild-type (FVB and NMRI) mice were from the Charles-River Laboratory. Animals were fed a standard chow diet (Safe). Throughout the study, the mice were housed with lights on from 7:00 am to 7:00 pm, and access to food and water was ad libitum.

*In vitro fertilization and embryo culture*. Eight- to twelve-week-old female FVB mice were superovulated by i.p. injection of 5 IU (0.1 ml) PMSG, followed 50 hours later by an i.p. injection of 5 IU (0.1 ml) of hCG.

Fourteen hours after hCG injection, cumulus-oocyte complexes were recovered from oviducts in HTF supplemented with 5 mg/ml of HSA. Spermatozoa were collected from the cauda epididymis of 10- to 14-week-old FVB mice and capacitated for 60 minutes in HTF/HSA medium at 37°C under a humidified atmosphere of 6% $CO_2$ in air. Oocytes were inseminated 14 hours after hCG injection with $10^6$ spermatozoa in HTF/HSA medium for 4 hours at 37°C in a $CO_2$-enriched (6%) atmosphere. Eggs were then transferred to 25 μl drops of G1 medium covered with paraffin oil. The embryo culture was conducted up to the blastocyst stage in sequential G1 and G2 medium preequilibrated at 37°C under the $CO_2$-enriched atmosphere. Embryos were kept in the G2 medium for 48 hours before the transfer to pseudopregnant females. The culture media used in these studies are largely used during ART in humans. For these studies, the ART procedure was repeated about 50 times, each time in a different animal.

*Embryo transfer*. NMRI females of at least 6 weeks of age were placed with vasectomized males to mate 2.5 days prior to embryo transfer. The morning after mating, females were checked for the presence of a vaginal plug. On the transfer day, pseudopregnant females were anesthetized by i.p. injection of xylazine (15 mg/kg) and ketamine (100 mg/kg). From 14 to 20 embryos were transferred to the uterus of each female.

Unless stated otherwise, 12- to 14-week-old male ART and control mice were used for all the in vitro and in vivo studies described below.

*Mesenteric artery function in vitro*. ART and control mice were killed with an overdose of pentobarbital sodium (200 mg/kg, i.p.). The mesenteric artery was dissected free of parenchyma and cut into a ring. Each ring was positioned between 2 stainless steel wires (diameter 25 μm) in a 5-ml organ bath of a small vessel myograph (DMT 610M; Danish Myo Technology) (30). The organ bath was filled with modified Krebs-Ringer bicarbonate solution (composition: 118.3 mM NaCl, 4.7 mM KCl, 2.5 mM $CaCl_2$, 1.2 mM $Mg2SO_4$, 1.2 mM $KH_2PO_4$, 25.0 mM $NaHCO_3$, and 11.1 mM glucose), maintained at 37 ± 0.5°C and aerated with 95% $O_2$ plus 5% $CO_2$ (pH = 7.4). At the beginning of the experiment, each vessel ring was stretched to its optimal resting tension corresponding to a transmural pressure of 100 mmHg and allowed to equilibrate for 1 hour. MyoDaq software (MyoDaq 2.01 M610; Danish Myo Technology) was used for data acquisition and display. Then, acetylcholine-induced (ACh, $10^{-9}$ to $10^{-5}$ M) or sodium nitroprusside–induced ($10^{-10}$ to $10^{-5}$ M) vasodilation was assessed in mesenteric arteries preconstricted with phenylephrine ($10^{-5}$ mol/l) at a level corresponding at least to the maximal response to potassium (100 mmol/l KCl). The ACh-induced change in tension was expressed as the percentage of the initial contraction induced by phenylephrine.

To assess arterial stiffness, the left carotid artery was quickly excised, placed in modified Krebs-Ringer solution (composition, see above) cleaned of adhering tissue and fat. The artery was then mounted onto a pressure myograph (Danish Myo Technology) in an organ bath filled with physiological buffer, as described previously (31). After a 30-minute equilibration period, the carotid artery was transilluminated under an inverted microscope (Zeiss Axio Vert A1) connected to a camera and a computerized system (MyoVIEW II Software; Danish Myotechnology) allowing the continuous recording of the artery diameter. Measurements of the inner and outer artery diameter were obtained during stepwise increases (10 mmHg steps for 5 minutes from 0 to 180 mmHg) of the intravascular pressure and expressed as a percentage of the baseline value measured at 10 mmHg of intravascular pressure.

*Arterial blood pressure*. Arterial blood pressure was recorded continuously in awake mice, as described previously (32). Briefly, a fluid-filled PE-10 tubing connected to a pressure transducer was inserted into the carotid artery under isoflurane anesthesia and tunneled subcutaneously to exit at the back of the neck. Mice were allowed to recover for 4–5 hours before the blood pressure measurement.

In additional ART and control mice, we measured arterial blood pressure by telemetry, as described previously (33). Briefly, blood pressure transmitters (TA11PA-C10 transmitter; DataSciences International) were implanted under inhalational anesthesia with isoflurane on a heating surface set at 36°C. Preoperatively, mice received 1 ml of prewarmed 0.9% saline i.p. to support fluid homeostasis and trimethoprim (6 mg/kg)/sulfadoxin (30 mg/kg) (Bactrim) s.c. for anti-infective prophylaxis. The left common carotid artery was exposed, and the tip of the telemetry catheter was inserted, advanced into the aortic arch, and secured by silk sutures. The body of the transmitter was positioned in an s.c. pocket on the right flank. Postoperatively, mice received s.c. injections twice per day for 7 days of flunixine (5 mg/kg body weight) for pain relief and 300 μl of glucose (5%) and 300 μl of normal saline (0.9%) to prevent exsiccosis.

From 10–12 days after implantation, transmitters were activated magnetically and offset-corrected blood pressure was recorded at 4-minute intervals for 48 consecutive hours. The recording room was maintained at 22–24°C with a 12-hour light/12-hour dark cycle, and mice had free access to food and water. The telemeter signal was processed using RPC-1 receivers, an APR-1 ambient pressure monitor,and a Dataquest A.R.T. 4.31 Gold acquisition system (DataSciences International).

*Histone deacetylase inhibitor administration*. To test for the potential pathogenic role of epigenetic mechanisms, sodium butyrate (2 mg/kg body weight/d in 200 μl of PBS, i.p.) was administered to 10-week-old male ART and control mice for 14 days.

*Methylation of imprinted genes in the aorta*. The maternally expressed paternally methylated *H19* (34) and *Gtl2* (35) genes and the paternally expressed maternally methylated *Peg3*, (36) *Peg1* (37), and *Snrpn* genes (38) were studied in the aorta. DNA was extracted using the QIAampDNA Microkit (Qiagen). Using the EZ Methylation Gold-Kit (Zymo Research), the extracted DNA was treated with sodium bisulfite in order to convert unmethylated cytosine residues to uracil. The converted DNA was eluted in 10 μl of TE buffer (10 mM Tris-HCl, 0.1 mM EDTA, pH 7.5). 2 μl of the bisulfite-treated DNA was used for subsequent PCR amplification.

The PCR amplifications were performed starting from 80–140 ng of bisulfite-treated DNA. All reactions were performed with PCR reaction mixtures (total volume 25 μl) containing oligonucleotides at 0.5 mM concentration and 12.5 μl of HotStarTaq Master Mix (Qiagen). The PCR conditions were the same for all 5 genes tested, i.e., 94°C for 15 minutes, followed by 40 cycles of 94°C for 30 seconds, 55°C for 30 seconds, 72°C for 30 seconds, and by a 72°C 10-minute final extension step. The characteristics of the amplicons and the oligonucleotides chosen have been described earlier (39).

The biotinylated PCR products were purified using streptavidin-sepharose beads (Amersham) and sequenced using the PSQ 96 Gold Reagent Kit (Biotage AB) with the following primers: H19: 5′-GTGTAAAGATTAGGGTTGT-3′; Gtl2: 5′-GTTATGGATTGGTGTTAAG-3′; Peg1: 5′-TCAATATCAACTAAATAATC-3′; Snrpn: 5′-GAATTGGAGTTGTGTGG-3′; Peg3: 5′-AATTGATAAGGTTGTAGATT-3′. The degree of methylation at each CpG site was determined using Pyro Q-CpG Software (Biotage AB). All samples were analyzed in duplicate. Diagrams showing the location of the DMDs and the DNA fragments of the 5 genes amplified by PCR in the present study have been published previously (39).

*Methylation of the eNOS gene promoter in the aorta*. Using the same methods, methylation analysis was performed in the eNOS (GenBank AF091262) core promoter, where DNA methylation was shown to control gene expression (19, 40). The following oligonucleotides were designed with the PyroMark Assay Design 2.0 program (Qiagen): eNOS-F: 5′-TGAGATTTTTGTGGTTATAGGAATATGAT-3′; eNOS-R: 5′-biotin-7CAACAAAATCCTAACCTTTTCCTTAA-3′. The biotinylated PCR products were purified using streptavidin-sepharose beads (Amersham) and sequenced using the PSQ 96 Gold Reagent Kit (Biotage AB) with the following oligonucleotide: eNOS-S: 5′-TTGGGTTTTTATTTATTAGTTTTA-3′. This sequence analyzed by pyrosequencing was 151-bp long, encompassing 8 CpGs.

*Protein extraction and eNOS Western blot*. Four carotid arteries of the same condition were pooled and grounded in liquid nitrogen. Each pool of carotid tissue was suspended in SDS lysis buffer (62.5 mM Tris, pH 6.8, 5% SDS, 10 mM EDTA). Following sonication and 5 minutes of full-speed centrifugation, supernatant proteins were quantified by the Lowry method. Samples were heated at 95°C for 3 minutes, loaded in duplicate (8 μg per well) in a 8% acrylamid gel, and transferred to PVDF membrane (Millipore). The membrane was blocked with 5% milk-TBS, 0.1% Tween (TBST) for 1 hour. Blots were probed with anti-eNOS (1:1000; BD Transduction

Laboratories) in 5% milk/TBST overnight and were detected using peroxidase-conjugated secondary antibody (1:10000) in 5% milk/TBST for 1 hour. Products were visualized by chemiluminescence (GE Healthcare), and band intensity was measured using ImageQuant 5.0 software (Molecular Dynamics). Equal protein loading was confirmed by β-actin (1:10000; Thermo Scientific Pierce Products) hybridization on the same membrane.

*RNA preparation and gene expression analysis*. Total RNA from aorta was extracted using the TRIzol RNA Isolation Reagents according to the manufacturer's protocol (Life Technologies Europe B.V.). From 500 to 1000 ng total RNA were reverse transcribed using 400 units of Moloney Murine Leukemia Virus Reverse Transcriptase (Invitrogen) in the presence of 1 U/μl RNasin (Promega Corp.), 0.2 μg of random primers (oligo[dN]6) (Promega Corp.), 2 mM dNTP, and 20 μM of DTT (Invitrogen). The expression of the cDNAs for mouse eNOS was determined by quantitative real-time PCR using an ABI StepOne Plus Sequence Detection System (Applera Europe) and normalized using the housekeeping gene Rps29. PCR products were quantified using Master SYBR Green Mix (Applera Europe), and results are expressed in AU relative to the control group mean value. Primers were designed using Primer Express software (Applera Europe) and chosen when possible on both sides of an intron to avoid amplification of eventual contaminating genomic DNA. Oligos were used at 217 nM each (Microsynth). The sequence of the primers used were as follows: eNOS, forward: 5′-AAGGCAGCGGTGGAAATTAA-3′; eNOS, reverse: 5′-TCACTTTGGCCAGCTGGTAAC-3′.

*Methylation of the endothelin-1 gene promoter in the aorta*. Methylation analysis was performed in the Edn-1 (GenBank NC_000079) promoter in a region where DNA methylation was shown to control gene expression (41, 42). The following oligonucleotides were designed with the PyroMark Assay Design 2.0 program (Qiagen): Edn-F: 5′-GTGATTTTTTA-AGGAGTTTTAGAAATAGG-3′; Edn-R: 5′-biotin-7AACCCTACAACCCTA-AACACACTTATT-3′. The biotinylated PCR products were purified using streptavidin-sepharose beads (Amersham) and sequenced using the PSQ 96 Gold Reagent Kit (Biotage AB) with the following oligonucleotide: Edn-S: 5′-GAGTTTTAGAAATAGGTAGG-3′. The sequence analyzed by pyrosequencing was 239-bp long, encompassing 9 CpGs.

*Methylation of the ACE gene promoter in the aorta*. Methylation analysis was performed in the ACE promoter, in a CpG island region where methylation was reported to be modified in the mouse fetus after maternal dietary changes during pregnancy (19, 40, 43). The following oligonucleotides were designed with the PyroMark Assay Design 2.0 program (Qiagen): ACE-F: 5′-biotin-7GGTGGTGGTTGGGTTTTATA-3′; ACE-R: 5′-CCCAACTAAC-CACCATACTCTAAAACAT-3′. The biotinylated PCR products were purified using streptavidin-sepharose beads (Amersham) and sequenced using the PSQ 96 Gold Reagent Kit (Biotage AB) with the following oligonucleotide: ACE-S: CCTCCACACTCCAATTATAACTTTC-3′. The sequence analyzed by pyrosequencing was 85-bp long, encompassing 10 CpGs.

*NO plasma concentration*. NO was measured in plasma samples obtained by cardiac punctuation by chemiluminescence with a NO analyzer (Sievers 280 NOA) after reduction of $NO_x$ to NO with $VCl_3$ (44).

*Survival*. Eighty male FVB mice generated by ART and 80 control mice born and raised in our animal facility were observed in these studies. Three to four animals were placed in a cage in the clean conventional mouse facility. Six ART and seven control mice had to be sacrificed because of injuries related to fighting. Throughout the study, the mice were housed with lights on from 7:00 am to 7:00 pm, and access to food and water was ad libitum. Thirty-two ART and twenty control mice were fed normal chow, 42 ART mice and 53 control mice were fed a HFD (49.5% fat, 31.5% protein, and 0% carbohydrates; Safe). One week each month, mice in the HFD groups were fed a standard chow diet (pellets) to avoid dental problems. Kaplan-Meier survival curves were constructed using known birth and death dates, and the log-rank test was used to evaluate statistical differences between groups.

*Statistics*. Statistical analyses were made using JMP v. 7.0 software (SAS Institute). Bivariate analyses were made using the unpaired 2-tailed Student's *t* test and 1- or 2-factor ANOVA. Post hoc comparisons were made using the Tukey HSD test and Dunnett's multiple comparison test. A *P* value of less than 0.05 was considered to indicate statistical significance. Unless otherwise indicated, data are given as mean ± SD.

*Study approval*. All animal protocols were approved by the CHUV Institutional Animal Care Committee.

## Acknowledgments

We are indebted to Françoise Urner for help with the initial studies and to Caroline Mathieu, Christelle Stouder, Pierre Dessen, and Arnaud Bichat for invaluable technical assistance. This work was supported by the Swiss National Science Foundation, the Eagle Foundation, the Leenaards Foundation, the FABER Foundation, the Swiss Society of Hypertension, the Prof. Dr. Max Cloetta Foundation, and the Placide Nicod Foundation.

Received for publication January 22, 2013, and accepted in revised form September 4, 2013.

Address correspondence to: Urs Scherrer, Swiss Cardiovascular Center Bern, University Hospital, Bern, Switzerland. Phone: 41.31.632.01.02; Fax: 41.31.632.42.11; E-mail: Urs.Scherrer2@insel.ch.

1. Barker DJ. Maternal and fetal origins of coronary heart disease. *J R Coll Physicians Lond*. 1994; 28(6):544–551.
2. Barker DJ. In utero programming of cardiovascular disease. *Theriogenology*. 2000;53(2):555–574.
3. Hakim TS, Mortola JP. Pulmonary vascular resistance in adult rats exposed to hypoxia in the neonatal period. *Can J Physiol Pharmacol*. 1990; 68(3):419–424.
4. Sartori C, Allemann Y, Trueb L, Delabays A, Nicod P, Scherrer U. Augmented vasoreactivity in adult life associated with perinatal vascular insult. *Lancet*. 1999;353(9171):2205–2207.
5. Jayet PY, et al. Pulmonary and systemic vascular dysfunction in young offspring of mothers with preeclampsia. *Circulation*. 2010;122(5):488–494.
6. Ceelen M, van Weissenbruch MM, Vermeiden JP, van Leeuwen FE, Delemarre-van de Waal HA. Cardiometabolic differences in children born after in vitro fertilization: follow-up study. *J Clin Endocrinol Metab*. 2008;93(5):1682–1688.
7. Watkins AJ, et al. Mouse embryo culture induces changes in postnatal phenotype including raised systolic blood pressure. *Proc Natl Acad Sci U S A*. 2007;104(13):5449–5454.
8. Scherrer U, et al. Systemic and pulmonary vascular dysfunction in children conceived by assisted reproductive technologies. *Circulation*. 2012;125(15):1890–1896.
9. Jarvisalo MJ, et al. Endothelial dysfunction and increased arterial intima-media thickness in children with type 1 diabetes. *Circulation*. 2004; 109(14):1750–1755.
10. Creager MA, Luscher TF, Cosentino F, Beckman JA. Diabetes and vascular disease: pathophysiology, clinical consequences, and medical therapy: Part I. *Circulation*. 2003;108(12):1527–1532.
11. Davis EF, et al. Cardiovascular risk factors in children and young adults born to preeclamptic pregnancies: a systematic review. *Pediatrics*. 2012; 129(6):e1552–e1561.
12. Kajantie E, Eriksson JG, Osmond C, Thornburg K, Barker DJ. Pre-eclampsia is associated with increased risk of stroke in the adult offspring: the Helsinki birth cohort study. *Stroke*. 2009; 40(4):1176–1180.
13. Rexhaj E, et al. Fetal programming of pulmonary vascular dysfunction in mice: role of epigenetic mechanisms. *Am J Physiol Heart Circ Physiol*. 2011;301(1):H247–H252.
14. De Rycke M, Liebaers I, Van Steirteghem A. Epigenetic risks related to assisted reproductive technologies: risk analysis and epigenetic inheritance. *Hum Reprod*. 2002;17(10):2487–2494.
15. Maher ER, Afnan M, Barratt CL. Epigenetic risks related to assisted reproductive technologies: epigenetics, imprinting, ART and icebergs? *Hum Reprod*. 2003;18(12):2508–2511.
16. Gluckman PD, Hanson MA, Beedle AS. Non-genomic transgenerational inheritance of disease risk. *Bioessays*. 2007;29(2):145–154.
17. Whitelaw NC, Whitelaw E. Transgenerational epigenetic inheritance in health and disease. *Curr Opin*

*Genet Dev*. 2008;18(3):273–279.
18. Weaver IC, et al. Epigenetic programming by maternal behavior. *Nat Neurosci*. 2004;7(8):847–854.
19. Chan Y, et al. The cell-specific expression of endothelial nitric-oxide synthase: a role for DNA methylation. *J Biol Chem*. 2004;279(33):35087–35100.
20. Rexhaj E, et al. Assisted reproductive technologies cause exaggerated diet-induced insulin resistance in mice. *FASEB J*. 2011;25:851.1.
21. Dansky HM, et al. Genetic background determines the extent of atherosclerosis in ApoE-deficient mice. *Arterioscler Thromb Vasc Biol*. 1999;19(8):1960–1968.
22. Shim J, Handberg A, Ostergren C, Falk E, Bentzon JF. Genetic susceptibility of the arterial wall is an important determinant of atherosclerosis in C57BL/6 and FVB/N mouse strains. *Arterioscler Thromb Vasc Biol*. 2011;31(8):1814–1820.
23. Vaissiere T, Sawan C, Herceg Z. Epigenetic interplay between histone modifications and DNA methylation in gene silencing. *Mutat Res*. 2008; 659(1–2):40–48.
24. Milutinovic S, D'Alessio AC, Detich N, Szyf M. Valproate induces widespread epigenetic reprogramming which involves demethylation of specific genes. *Carcinogenesis*. 2007;28(3):560–571.
25. Ou JN, et al. Histone deacetylase inhibitor Trichostatin A induces global and gene-specific DNA demethylation in human cancer cell lines. *Biochem Pharmacol*. 2007;73(9):1297–1307.
26. Gluckman PD, Hanson MA, Buklijas T, Low FM, Beedle AS. Epigenetic mechanisms that underpin metabolic and cardiovascular diseases. *Nat Rev Endocrinol*. 2009;5(7):401–408.
27. Santos MA, Kuijk EW, Macklon NS. The impact of ovarian stimulation for IVF on the developing embryo. *Reproduction*. 2010;139(1):23–34.
28. Market-Velker BA, Fernandes AD, Mann MR. Side-by-side comparison of five commercial media systems in a mouse model: suboptimal in vitro culture interferes with imprint maintenance. *Biol Reprod*. 2010;83(6):938–950.
29. Rexhaj E, Rimoldi S, Giacobino A, Sartori C, Allemann Y, Scherrer U. Epigenetically-induced systemic vascular dysfunction and hypertension by in vitro fertilization; prevention by addition of melatonin to the culture media. *FASEB J*. 2012;26:874.5.
30. Mulvany MJ, Halpern W. Contractile properties of small arterial resistance vessels in spontaneously hypertensive and normotensive rats. *Circ Res*. 1977;41(1):19–26.
31. Faury G, et al. Developmental adaptation of the mouse cardiovascular system to elastin haploinsufficiency. *J Clin Invest*. 2003;112(9):1419–1428.
32. Cook S, et al. Partial gene deletion of endothelial nitric oxide synthase predisposes to exaggerated high-fat diet-induced insulin resistance and arterial hypertension. *Diabetes*. 2004;53(8):2067–2072.
33. Schuler B, Rettich A, Vogel J, Gassmann M, Arras M. Optimized surgical techniques and postoperative care improve survival rates and permit accurate telemetric recording in exercising mice. *BMC Vet Res*. 2009;5:28.
34. Tremblay KD, Duran KL, Bartolomei MS. A 5′ 2-kilobase-pair region of the imprinted mouse H19 gene exhibits exclusive paternal methylation throughout development. *Mol Cell Biol*. 1997; 17(8):4322–4329.
35. Li JY, Lees-Murdock DJ, Xu GL, Walsh CP. Timing of establishment of paternal methylation imprints in the mouse. *Genomics*. 2004;84(6):952–960.
36. Kuroiwa Y, et al. Peg3 imprinted gene on proximal chromosome 7 encodes for a zinc finger protein. *Nat Genet*. 1996;12(2):186–190.
37. Kaneko-Ishino T, et al. Peg1/Mest imprinted gene on chromosome 6 identified by cDNA subtraction hybridization. *Nat Genet*. 1995;11(1):52–59.
38. Shemer R, Birger Y, Riggs AD, Razin A. Structure of the imprinted mouse Snrpn gene and establishment of its parental-specific methylation pattern. *Proc Natl Acad Sci U S A*. 1997;94(19):10267–10272.
39. Stouder C, Deutsch S, Paoloni-Giacobino A. Superovulation in mice alters the methylation pattern of imprinted genes in the sperm of the offspring. *Reprod Toxicol*. 2009;28(4):536–541.
40. Fish JE, et al. The expression of endothelial nitric-oxide synthase is controlled by a cell-specific histone code. *J Biol Chem*. 2005;280(26):24824–24838.
41. Aitsebaomo J, Kingsley-Kallesen ML, Wu Y, Quertermous T, Patterson C. Vezf1/DB1 is an endothelial cell-specific transcription factor that regulates expression of the endothelin-1 promoter. *J Biol Chem*. 2001;276(42):39197–39205.
42. Stow LR, Jacobs ME, Wingo CS, Cain BD. Endothelin-1 gene regulation. *FASEB J*. 2011;25(1):16–28.
43. Goyal R, Goyal D, Leitzke A, Gheorghe CP, Longo LD. Brain renin-angiotensin system: fetal epigenetic programming by maternal protein restriction during pregnancy. *Reprod Sci*. 2010;17(3):227–238.
44. Duplain H, et al. Insulin resistance, hyperlipidemia, and hypertension in mice lacking endothelial nitric oxide synthase. *Circulation*. 2001;104(3):342–345.